

New measurement of the β - γ directional correlation in ^{22}Na

C. J. Bowers, S. J. Freedman, B. Fujikawa, A. O. Macchiavelli, R. W. MacLeod, J. Reich, S. Q. Shang, P. A. Vetter, and E. Wasserman

Lawrence Berkeley National Laboratory, University of California, Berkeley, California 94720
and Physics Department, University of California, Berkeley, California 94720

(Received 19 December 1997)

We have measured the β - γ directional correlation coefficient A_{22} in the decay of ^{22}Na to the 2^+ 1275 keV excited state of ^{22}Ne . We find $A_{22} = (5.3 \pm 2.5) \times 10^{-4}$. This measurement has higher precision but disagrees with most previous experiments. The value for A_{22} , combined with other experimental inputs, gives recoil-order form factors in disagreement with theoretical estimates. This experiment demonstrates the capabilities of Gammasphere as an instrument for precise β - γ correlation measurements. [S0556-2813(99)01702-1]

PACS number(s): 23.40.-s, 23.20.En, 27.30.+t

I. INTRODUCTION

The allowed approximation description of nuclear β decay accounts for only the $l=0$ part of the lepton current. In this approximation, there is no β - γ directional correlation. Interference between allowed and higher-order matrix elements ($l \neq 0$) leads to nonzero directional correlations. However, the correlation is suppressed by the ratio of forbidden to allowed matrix elements, typically 10^{-5} . With suppressed allowed matrix elements, the β - γ directional correlation may be larger. The β^+ decay of ^{22}Na to the 1275 keV excited state of ^{22}Ne ($3^+ \rightarrow 2^+$) (see Fig. 1) proceeds by allowed Gamow-Teller decay. However, the large $\log ft$ value of this decay (7.42) indicates a suppression of ~ 100 . If the mechanism responsible for the suppression of the allowed matrix element does not also reduce the relevant forbidden matrix elements, then the β - γ directional correlation should be $\sim 10^{-3}$.

The large $\log ft$ value for ^{22}Na has stimulated interest in observing and constraining second-order corrections to the decay (Refs. [1–6]). Measurements of the electron capture to β^+ -decay branching ratio (ϵ/β^+) disagree with allowed-order calculations [6], suggesting that higher order matrix elements in ^{22}Na are large. For example, Firestone *et al.* [5] have shown that the inclusion of large higher order matrix elements in the calculation of ϵ/β^+ can remove the discrepancy between experiment and theory, while Skalsey *et al.* [7] argued that corrections beyond second order in recoil are probably negligible. Kunze *et al.* [6] concluded that the discrepancy between the measured ϵ/β^+ with allowed-order calculations remained significant. Large second-order terms would result in a large β - γ directional correlation or other observables. Precise measurements of these observables constrain second-order fundamental form factors of β decay, including those related to so-called second-class current contributions to hadronic weak interactions [8,9]. The accessibility of other observables of interest in the $^{22}\text{Na}(3^+) \rightarrow ^{22}\text{Ne}(2^+)$ system, from which one can construct a complete set of form factors for the decay and thus infer forbidden order contributions motivates our experiment. Moreover, the existence of inconsistent but precise measurements of the ^{22}Na angular correlation (see Table II) invites a resolution.

Second-class terms are expected to be zero from symmetry arguments, but isospin symmetry breaking can result in small second-class induced tensor currents [10]. Limits on the existence of second-class currents derive from measurements in the $A=12$ isotriplet of the β^+ directional correlation with aligned nuclei using contributions from weak magnetism terms from other observables [11–15]. The most recent measurements in $A=12$ by Minamisono *et al.* have indicated a small but nonzero second-class induced tensor term $+0.01 < 2Mf_T/f_a < +0.43$. Constraining second-class terms using only observables in ^{22}Na requires calculations of first-class contributions to induced terms, and a complete set of complementary measurements to constrain the forbidden-order form factors.

II. THE β - γ ANGULAR CORRELATION

In this experiment we measure a correlation of the form

$$W(\theta) \propto 1 + \frac{3}{2} A_{22} \cos^2 \theta, \quad (2.1)$$

where $|A_{22}| \ll 1$, and θ is the angle between the β^+ and the subsequent γ -ray momenta. Using the expansion in Ref. [5]

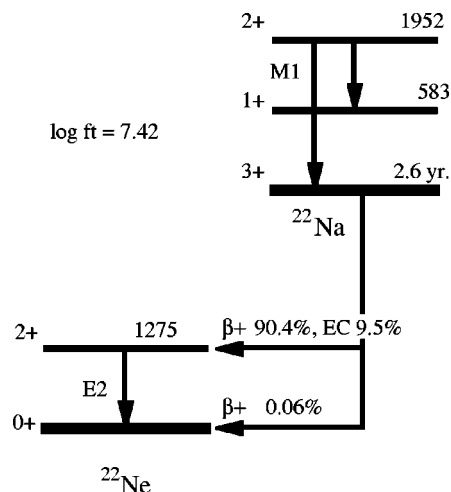


FIG. 1. Decay scheme of ^{22}Na , energies in keV.

$$\begin{aligned}
A_{22} &= -\frac{E}{21Mc_1} \left(c_1 - b - d + \frac{8}{3} c_2 M(E_0 - E) c_1 \right) \\
&\approx \left(5.1 \frac{b}{Ac_1} E + 5.1 \frac{d}{Ac_1} E - 3.5 \frac{c_2}{c_1 R^2} E(E_0 - E) \right) \\
&\quad \times 10^{-5} \text{ MeV}^{-1}, \tag{2.2}
\end{aligned}$$

where E (E_0) is the total (maximum) energy of the β particle ($E_0 = 1056$ keV), M is the nuclear mass, R is the nuclear radius, and A is the nucleon number. The form factors c , b , and d are associated with the Gamow-Teller, weak magnetism, and induced tensor matrix elements. To this order, it is sufficient to retain the momentum-transfer (q) dependence only for the Gamow-Teller form factor, defining $c(q^2) \equiv c_1 + c_2 q^2 + \dots$. In principle, a measurement of A_{22} as a function of the β^+ energy can distinguish the relative contribution of c_2 from that of b and d .

To measure A_{22} , we used the Gammasphere array at the 88-inch Cyclotron at Lawrence Berkeley National Laboratory. Gammasphere is a spherical array of Compton-suppressed Ge detectors into which we inserted a ^{22}Na source and a β detector, in order to detect coincidences between the β detector and 1275 keV γ rays in each Ge detector. To normalize the coincidence counts accounting for the different Ge detector efficiencies which vary by $\sim 20\%$, we also collected single 1275 keV γ rays for each detector. The number of singles counts for a Ge detector at angle θ relative to the β detector, $N_s(\theta) = \epsilon(\theta) N'_s(\theta)$, where $N'_s(\theta)$ is the number of γ rays emitted in direction θ and $\epsilon(\theta)$ is the efficiency of the Ge detector at angle θ . Similarly, $N_c(\theta) = \epsilon(\theta) N'_c(\theta)$ for coincidence counts. Then the ratio of coincidences to singles is

$$\frac{N_c(\theta)}{N_s(\theta)} = \frac{\epsilon(\theta) N'_c(\theta)}{\epsilon(\theta) N'_s(\theta)} = \frac{N'_c(\theta)}{N'_s(\theta)} \propto W(\theta). \tag{2.3}$$

We have assumed that $\epsilon(\theta)$ is the same for singles and coincidence counts. We determine A_{22} from a fit of the coincidence-to-singles ratio as a function of detector angle θ .

III. DETECTORS

During the experiment, Gammasphere was configured with 100 Compton-suppressed Ge detectors [16,17]. The Ge detectors occupy (at most) 110 hexagonal surfaces of a 122-element polyhedron surrounding an 18 cm radius target chamber. The 12 pentagonal surfaces of the polyhedron are used for entrance and exit beam ports (not used in this experiment), or for additional detectors.

Each Ge detector assembly is a cylindrical Ge detector surrounded by six bismuth germanate (BGO) scintillators on the sides and one BGO scintillator in back. The BGO detectors are normally used to improve the photopeak to Compton-scattered ratio in the Ge detector spectrum by operating them in anticoincidence. In this experiment, however, the BGO detectors were not used, since the γ ray of interest (1275 keV) has negligible background from Compton scattering of γ rays of higher energy, as illustrated in Fig. 2. Moreover, it is essential to avoid detector-dependent varia-

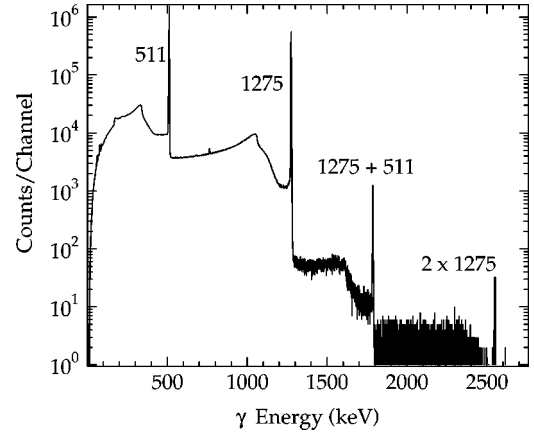


FIG. 2. Single γ event energy spectrum summed for all Ge Gammasphere detectors.

tions in the full-energy coincidence to singles efficiency. In coincidence events, the positron normally annihilates in the β detector, while in singles events, the positron is more likely to have annihilated at the inner surface of the vacuum chamber. The difference in triggering and event rejection could cause a systematic difference between the coincidence and singles efficiency. The BGO detectors were disabled by turning off the photomultiplier tubes' high voltage supply.

Each ~ 7 cm dia. \times 8 cm Ge detector is 25 cm from the ^{22}Na source, subtending 0.5% solid angle, and the probability for a 1275 keV γ ray which hits a detector to deposit its full energy is roughly 25%. Therefore, each Ge detector has $\sim 0.1\%$ probability of absorbing the full energy of a γ ray coming from the center of the array. The full width at half maximum (FWHM) of the full energy peak is typically 2.3 keV. Annihilation photons at 511 keV are completely resolved. Annihilation in-flight photons at 1275 keV are a negligible contribution.

To measure an event in a Ge detector, a fast linear signal from a Ge detector is discriminated, adding a constant voltage pulse to an analog sum bus. An adjustable discriminator on the bus sets the minimum multiplicity of Ge detector hits required to trigger an event acquisition. The threshold was one or more Ge detector hits, forming the pretrigger. After a pretrigger is generated, the slow Ge detector signals are digitized with 14-bit resolution. A constant fraction discriminator on each detector signal also provides the start signal for a time to amplitude converter (we call this signal GeTAC). Each GeTAC receives a stop signal from the delayed pretrigger signal.

The ^{22}Na source and the β detector were inserted into the center of the Gammasphere array through the access port at 27° relative to the beamline. The angular position of the β detector is known to about 2° , and the associated fractional systematic error in A_{22} is $< 0.1\%$. The β detector is a 3 mm thick \times 12.5 mm diameter disk of Bicron 404 plastic scintillator attached to a Hamamatsu R1450 photomultiplier tube (PMT). The 6 μCi source was deposited from NaCl solution onto a 1 mm spot and sandwiched between two 1 mg/cm 2 Kapton foils [18,19]. The source was mounted on a nylon fixture 10.7 mm from the end of the scintillator. According to Monte Carlo simulations, this source to detector distance optimizes high β detector solid angle versus

finite detector size. The source was centered in the Gamma-sphere array to within 0.5 mm. This position uncertainty corresponds to a 4% uncertainty in A_{22} . The solid angle subtended by the β detector is $\sim 6\%$ of 4π . The thickness of the scintillator was chosen to stop β^+ particles with maximum energy (546 keV), while minimizing the Compton scattering background from 511 keV γ rays.

A LeCroy fast encoding and readout ADC (FERA) digitized the β detector signal. The FERA was gated by a coincidence between a discriminated β detector pulse and the pretrigger from the Ge array. The delays and gate widths were chosen so that the timing of the FERA gate was determined only by the β detector signal. This was required because the timing of the pretrigger relative to the β detector signal varies by up to 20 ns, depending on which Ge detector generated the pretrigger. Gating the FERA with the Ge pretrigger alone would result in systematically different β energy spectra associated with each Ge detector. For events with no β signal, the FERA is gated by the Ge pretrigger alone. This arrangement makes singles and coincidence events appear identical to the downstream data acquisition electronics, avoiding possible systematic differences in the readout process. The level discriminator on the β signal also starts a TAC (β TAC), which is stopped by the delayed pretrigger signal.

For each hit Ge detector, the digitized energy, the GeTAC value, and a detector identifier are recorded. For each event, the beta energy and β TAC are also included. For events with no detected β , the beta energy is at the pedestal of the FERA. Each event is processed on-line by a ‘‘farm’’ of crate-based processors which apply energy and timing corrections to the Ge detector data. The data stream was written to several 8 mm tapes in parallel for off-line data sorting. The deadtime was $\sim 15 \mu\text{s}$, and with the $6 \mu\text{Ci}$ source used here, the measurement was count rate limited.

IV. ANALYSIS

The results presented here are based on data runs in January and June of 1997, with a total of 9 days of data acquisition. Approximately 8×10^9 events were written to tape, with 4.5×10^9 photopeak 1275 keV γ 's. To reduce the amount of data written to tape, we used online Gammasphere event processing to reject events without at least one γ with energy above ~ 1000 keV.

For each detector, coincident β - γ and single γ events are selected in the off-line analysis. We identify photopeak 1275 keV γ 's within a 10 keV energy window for both coincidences and singles. For singles counts, the 1275 keV γ is required to be in prompt coincidence with the pretrigger. This requirement is enforced by placing a cut on GeTAC, illustrated in Fig. 3. Coincidence γ counts are identified by making the same cut on GeTAC, and a cut on the difference between GeTAC and the β -TAC, in order to select γ 's accompanied by prompt β 's. We use the difference (GeTAC- β TAC) to eliminate Ge detector dependent timing offsets in the β TAC value. The energy of the β is required to be in the range of ~ 120 –505 keV. This eliminates a low-energy background in the β^+ spectrum and spurious high-energy counts above the end-point energy. The measured β energy spectrum is shown in Fig. 4. Accidental β - γ coinci-

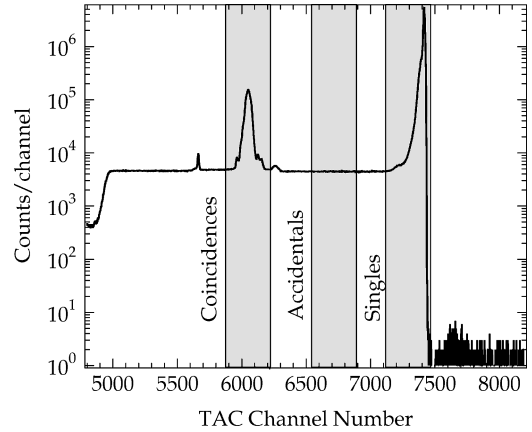


FIG. 3. Time spectrum summed for all γ detectors generated by subtracting β TAC from GeTAC for all γ events. Prompt singles and coincidence event windows are shown in shaded bars. The small peak to the left of the coincidence window is caused by digital overflow in the β TAC spectrum (shifted by the subtraction) and the small peak just outside the coincidence window to the right is generated by three germanium detectors with anomalously slow timing response (removed from the final analysis).

dences are subtracted based on an equal-length timing window on the GeTAC- β TAC spectrum shown in Fig. 3.

The angular correlation coefficient is determined by fitting the ratios for each detector to the linear function $N_c(\theta)/N_s(\theta) = R + a \cos^2 \theta$ (where θ is the included angle between the β and γ detectors), minimizing χ^2 to extract a . Geometric corrections described below are applied to a yielding A_{22} . Figure 5 shows all of the data binned by common detector angles with the best fit $(N_c(\theta)/N_s(\theta) - R)/R = (a/R) \cos^2 \theta$ function for the January and June data sets. To arrive at our final value of A_{22} , the data were averaged by calculating a/R for each of the 15 individual data tapes per run and averaging the results. Statistical uncertainty for each detector per tape is derived from the number of counts observed. The statistical error on the tape-averaged a/R derived from this procedure is increased by $\sqrt{\chi^2}$ to account for an elevated reduced χ^2 of ~ 1.4 for the distribution of a/R among 15 tapes. This scatter is larger than expected, but consistent with a time drift in the extracted R term, although

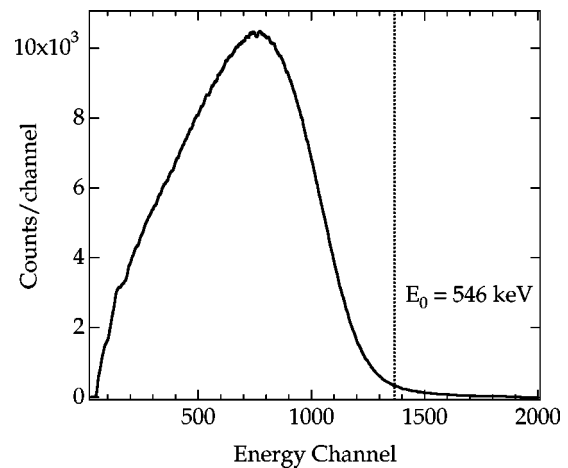


FIG. 4. β^+ energy spectrum for events with a coincident 1275 keV γ . Energy uncertainty is about 8 keV.

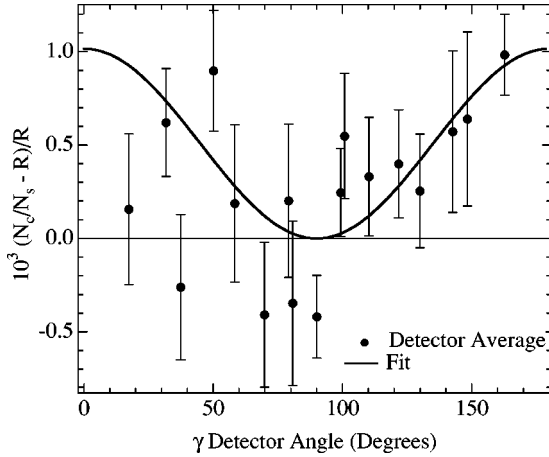


FIG. 5. Averaged coincidence/singles ratio as a function of γ detector angle in the array—Ge detectors at the same angle have been binned together for both data runs. The constant term R (see main text) has been subtracted and the data normalized to R to exhibit the angular dependence more clearly.

a linear drift in time of a/R is not statistically resolved in our data. We observe a resolved time drift in the constant rate term R of 0.3% among the tapes in the June run, likely caused by time drifts in triggering electronics among the γ detectors or gain drift in the β detector photomultiplier tube. Any systematic shift in a/R caused by the time drift in R should be accounted for within our renormalized statistical uncertainty.

We performed an additional analysis on the June 1997 data set in which the β energy spectrum was divided into four equal statistics bins. We calculated $(N_c/N_s)(\theta)$ for each bin, using only 1275 keV γ events coincident with a β^+ of appropriate energy. The results for the extracted A_{22} for each energy range are shown in Table I with statistical errors given for each energy bin. The energy scale uncertainty is 8 keV per bin. Systematic uncertainty for each A_{22} is 0.5×10^{-4} . These results are consistent with the linear dependence of A_{22} on β^+ energy predicted by Eq. (2.2), but the statistical errors are large.

The data acquired in January 1997 is not used for the β energy-dependent analysis. For this run, the FERA digitizing the β energy signal was gated with the delayed Ge pretrigger alone, resulting in slightly different β energy spectra for coincidences with different Ge detectors, as discussed in the previous section. It is still possible to use the data from January 1997 for a full-spectrum A_{22} by using only the level discriminator to determine whether or not a β of sufficient energy had hit the detector. For this data, the digitized β energy was ignored.

TABLE I. Measured A_{22} values for different β energy bins. Energy uncertainty for each bin is 8 keV and only statistical errors are shown for A_{22} . Systematic error for each bin is 0.5×10^{-4} .

β^+ Energy (keV)	$A_{22}(\times 10^{-4})$
110–216	4.2 ± 6.0
216–291	4.0 ± 6.0
291–361	-2.3 ± 6.1
361–505	12.3 ± 6.1

V. CORRECTIONS

To extract A_{22} , we correct for the solid angles of β and γ detectors. We apply an angular correction factor $Q_{2\beta} \cdot Q_{2\gamma}$ to our fit-extracted $\cos^2 \theta$ term a

$$A_{22} = a / (Q_{2\beta} Q_{2\gamma}), \quad (5.1)$$

where $Q_{2\gamma}$ and $Q_{2\beta}$ are the convolution of the angular correlation and detector angle. For our geometry inside Gamma-sphere, the product $Q_{2\beta} \cdot Q_{2\gamma} = 0.736 \pm 0.029$ where the uncertainty results from the spatial variation of the β detector efficiency across the surface of the detector (depending on incident positron angle and energy) by an estimated 20%; and the 0.5 mm measurement uncertainty of the diameter and position of the β detector relative to the source.

Angular anisotropy introduced by β^+ scattering from the source holder material should increase the effective solid angle of the β detector by roughly 1%. β^+ scattering from the aluminum Gamma-sphere target chamber is estimated to produce a count rate 10^{-4} times the unscattered rate. For the 3 mm thick β detector, the ratio of events where a 511 keV annihilation photon triggers the detector to true β events can be estimated to be roughly 1.5×10^{-4} , thus negligible in extracting the coincidence/singles ratio.

A correction for background under the 1275 keV photopeak in the coincidence/singles ratio amounted to roughly 10^{-3} of the ratio in early an analysis of a subset of the data, and thus was ignored in our final analysis. Measured background count rates under the photopeak would extrapolate to a background rate during the data run. The background rate during the run was roughly 2×10^{-3} times the singles rate. Fitting the angular dependence of the background 1275 keV γ data in the array yielded a $\cos^2 \theta$ angular correlation parameter with the β detector direction of 0.022(9), so the projection of background counts to the measured A_{22} would be at most $(2 \times 10^{-3}) \times 0.022 = 4.4 \times 10^{-5}$, substantially smaller than our statistical error. The observed angular correlation from the background data is caused by five γ detectors in the forward beam direction with 1275 keV rates five times higher than the rest of the detectors in the array, probably due to ^{22}Na activation of the aluminum target chamber in this region. Eliminating these detectors from the analysis resulted in a change of our A_{22} value of only 2×10^{-5} .

Seven of the 100 operational Ge detectors were left out of our analysis. In four cases, the FWHM of the 1275 keV peak was anomalously large and showed a low-energy tail characteristic of radiation damage. For three other detectors, the GeTAC- β TAC spectrum had coincidence timing peaks roughly three times as wide as the other detectors.

For the data set taken in June 1997, the coincidence/singles ratios among the detectors yield an angular correlation (corrected for solid angle) of $A_{22} = (3.4 \pm 3.3) \times 10^{-4}$ (statistical error only). The January 1997 data yield $A_{22} = (7.5 \pm 3.6) \times 10^{-4}$ (statistical error only). Averaging together the two data sets, we obtain $A_{22} = (5.3 \pm 2.4 \pm 0.5) \times 10^{-4}$, where the first error is statistical and the second

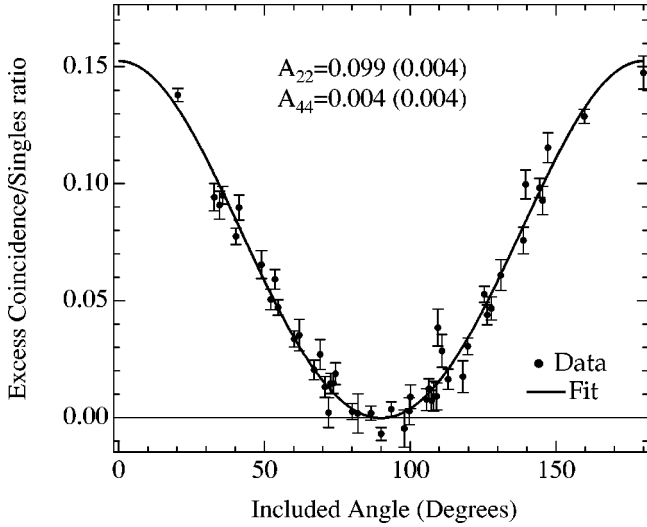


FIG. 6. Coincidence/singles ratio as a function of included angle between detector pairs for 1173/1332 keV γ coincidences from ^{60}Ni . Ge detector pairs with similar angles have been binned together for clarity.

systematic. The systematic uncertainty stems from background subtraction and solid angle correction uncertainty described above.

As a test of our technique, we also measured the well-known γ - γ angular correlation in ^{60}Co . A 10 μCi ^{60}Co source was used with 92 Ge detectors. The trigger was a single Ge detector hit, and $\sim 2.5 \times 10^8$ events were written to tape. For each detector, 1173 and 1332 keV γ ^{60}Ni photopeaks were defined with 10 keV energy windows and the requirement of a prompt coincidence with the triggering γ ray. For each of the ~ 8000 pairs of detectors, the number of coincidences between an 1173 keV γ in one and a 1332 keV γ in the other were divided by the product of the singles counts. The average coincidence to singles ratio is plotted versus the included angle between detector pairs as shown in Fig. 6. Pairs of detectors with similar included angle have been binned together. For the γ - γ angular correlation in ^{60}Ni , we measure $A_{22} = (0.099 \pm 0.004)$, (statistical uncertainty) compared to the expected theoretical value of 0.1020 from Ref. [20], and the experimental value $A_{22} = (0.1010 \pm 0.0011)$ measured in Ref. [21]. Our value $A_{44} = (0.004 \pm 0.004)$ is consistent with the theoretical value of 0.009 [20], and the measured $A_{44} = (0.0092 \pm 0.0007)$ [21].

VI. DISCUSSION

Previous measurements of A_{22} for ^{22}Na are shown in Table II and in Fig. 7. Our results differ significantly from several measurements with comparable stated precision, most strongly disagreeing with experiments described in Refs. [1] and [2]. One source of systematic error in these measurements is the prompt summing of the 1275 and 511 keV γ 's. 511 keV γ 's are produced when positrons annihilate in the β detector, creating a false angular correlation. Measurements of A_{22} with absorbers of varying thickness were used to extrapolate to an ideal large absorber thickness where the effect of the 511 keV γ summing is negligible, but the corrections applied to the results were large compared to A_{22} .

TABLE II. Measured values of ^{22}Na β - γ directional correlation A_{22} .

Author	$A_{22}(\times 10^{-3})$	E_{β} (keV)
Steffen (1959) [1]	-1.8 ± 0.3	350
Daniel and Eakins (1960) [24]	-20.0 ± 2.0	
Subba Rao (1961) [25]	-15.0 ± 3.0	120-450
Grabowski <i>et al.</i> (1965) [26]	-1.0 ± 5.0	400
Müller (1965) [2]	-0.3 ± 0.5	140-250
Müller (1965) [2]	-0.3 ± 0.4	250-480
Sastry <i>et al.</i> (1968) [27]	-1.0 ± 1.2	400
This result	0.53 ± 0.25	120-505

In our measurement this extrapolation is unnecessary. The use of 100 independent detectors greatly reduces the prompt summing effects while still maintaining high detection efficiency. In addition, the high resolution of Ge detectors, as opposed to NaI detectors used in the previous measurements, reduces the effect of summing in to the 1275 keV photopeak. Finally, the position of the β detector is such that it is still roughly in the geometrical center of the Ge array. Therefore, positron annihilation in the β detector results in essentially isotropic distribution of 511 keV γ 's in the Ge array. Using Gammasphere, prompt summing has a negligible effect on the measured asymmetry.

Our measurement of A_{22} , combined with existing results for other ^{22}Na observables gives values for the form factors of interest, which can be compared with shell-model based calculations from Ref. [7] using matrix elements calculated in Ref. [22]. Reference [5] describes the dependence of the various accessible observables on the form factors, which we summarize here:

$$R = 1 - (1.56B - 0.7D + 0.0013H + 18.0C_2) \times 10^{-3}, \tag{6.1}$$

$$S = -(1.79B - 0.17D + 0.00074H - 7.78C_2) \times 10^{-3} \text{ MeV}^{-1}, \tag{6.2}$$

$$P_L = 1 - (2.46B - 0.13C_2 + 1.23D + 0.0039H) \times 10^{-4} \beta, \tag{6.3}$$

$$A_{22} = (4.4B + 4.4D - 0.6C_2) \times 10^{-5}. \tag{6.4}$$

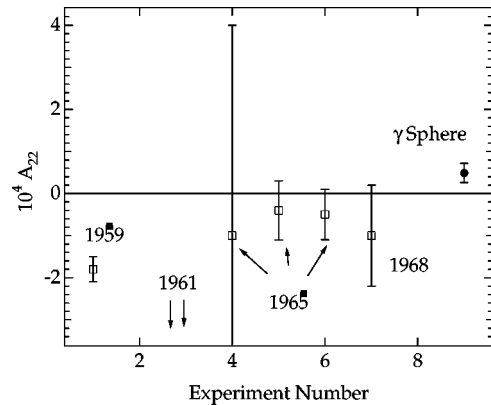


FIG. 7. Comparison of our measurement of A_{22} (circle) with earlier experiments (squares) listed in Table II.

The observables are respectively the skew ratio of the measured ϵ/β^+ rate to allowed order theory (R), the shape factor of the β^+ spectrum (S), the longitudinal polarization of the emitted β^+ (P_L), and the β - γ angular correlation (evaluated at a total β^+ energy of 850 keV). The dependence of the recoil order form factors is exhibited, with the reparametrization $B \equiv b/Ac_1$, $D \equiv d/Ac_1$, $C_2 \equiv c_2/Rc_1$, $H \equiv h/A^2c_1$, with R the nuclear radius, A the nucleon number, h the induced pseudoscalar form factor, and c_1 and c_2 the terms in the recoil order expansion of the Gamow-Teller coupling.

The value of A_{22} depends most strongly on the weak magnetism and the induced tensor terms, B and D , respectively. The value of the weak magnetism form factor in the decay can be fixed by the measured value of the width of the analog $M1$ ($2^+ \rightarrow 3^+$) transition in ^{22}Na , $\Gamma_{M1} = 3.6(1.7) \times 10^{-4}$ eV [23]. This result, together with a theoretical bias for a negative value of B from Refs. [23] and [7], implies $B = -14(4)$. We can then extract $D = 26(7)$ from our measured A_{22} . Although the choice of experimental inputs to determine all of the form factors is problematic, our determination of D is nearly independent of contributions from observables other than A_{22} , Γ_{M1} , and $\log ft$. This result is to

be compared with the calculation of the first-class part of $D = 2.5$ with an estimated uncertainty of 20% in Ref. [7]. In principle, this disagreement with the prediction of D could be attributed to a large second-class current contribution, but this amplitude of second-class tensor interaction is strongly excluded by the $A = 12$ experiments [11]. Therefore, it seems more likely that either the theoretical estimate of the first-class part of D , or the extraction of the weak magnetism term B from Γ_{M1} is incorrect. More precise measurements of Γ_{M1} from the ($2^+ \rightarrow 3^+$) branching ratio, as well as reassessment of the calculated transition matrix elements are required. To establish a more reliable set of form factors, our group is pursuing a magnetic spectrometer measurement of the shape factor of the β spectrum in ^{22}Na as well as a new Γ_{M1} measurement.

ACKNOWLEDGMENTS

We would like to acknowledge the assistance of the technical staff at the 88-inch Cyclotron. This work was supported by the Director, Office of Energy Research, Office of Basic Energy Sciences, of the U.S. Department of Energy under Contract No. DE-AC03-76SF00098.

-
- [1] R. M. Steffen, Phys. Rev. Lett. **3**, 277 (1959).
 - [2] H. Müller, Nucl. Phys. **74**, 449 (1965).
 - [3] R. B. Firestone, R. A. Warner, W. C. McHarris, and W. H. Kelly, Phys. Rev. Lett. **35**, 713 (1975).
 - [4] H. Wenninger, J. Stiewe, and H. Leutz, Nucl. Phys. **A109**, 561 (1968).
 - [5] R. B. Firestone, W. C. McHarris, and B. R. Holstein, Phys. Rev. C **18**, 2719 (1978).
 - [6] V. Kunze, W.-D. Schmidt-Ott, and H. Behrens, Z. Phys. A **337**, 169 (1990).
 - [7] M. Skalsey, T. A. Girard, D. Newman, and A. Rich, Phys. Rev. Lett. **49**, 708 (1985).
 - [8] B. R. Holstein, Rev. Mod. Phys. **46**, 789 (1974).
 - [9] L. Grenacs, Annu. Rev. Nucl. Part. Sci. **35**, 455 (1985).
 - [10] B. M. K. Nefkins, G. A. Miller, and I. Slaus, Comments Nucl. Part. Phys. **20**, 221 (1992).
 - [11] T. Minamisono, K. Matsuta, T. Yamagachi, K. Minamisono, T. Ikeda, Y. Muramoto, M. Fukuda, and Y. Nojiri, Nucl. Instrum. Methods Phys. Res. A **402**, 218 (1998).
 - [12] K. Matsuta, T. Minamisono, Y. Nojiri, M. Fukuda, T. Onishi, and K. Minamisono, Nucl. Instrum. Methods Phys. Res. A **402**, 229 (1998).
 - [13] Y. Masuda, T. Minamisono, Y. Nojiri, and K. Sugimoto, Phys. Rev. Lett. **43**, 1083 (1979).
 - [14] P. Lebrun *et al.*, Phys. Rev. Lett. **40**, 302 (1979).
 - [15] H. Brandle *et al.*, Phys. Rev. Lett. **41**, 299 (1978).
 - [16] I.-Y. Lee, Nucl. Phys. **A520**, 641c (1990).
 - [17] A. M. Baxter *et al.*, Nucl. Instrum. Methods Phys. Res. A **317**, 101 (1992).
 - [18] Isotope Products Laboratories, Pasadena, CA.
 - [19] J. Reich, Diplom Thesis, TU Munich, 1996.
 - [20] H. Appel, *Numerical Tables for Angular Correlation Computations in α -, β -, and γ -Spectroscopy: 3j-, 6j-, 9j-Symbols, F- and Γ -Coefficients*, Landholt-Börnstein New Series I/3 (Springer, New York, 1968).
 - [21] H. Appel, H. Behrens, K. Bürk, H. W. Müller, L. Szybisz, and R. Wishhusen, Z. Phys. **268**, 347 (1974).
 - [22] B. A. Brown and B. H. Wildenthal, Phys. Rev. C **27**, 1296 (1983).
 - [23] R. B. Firestone, L. H. Harwood, and R. A. Warner, University of California, Lawrence Berkeley Laboratory Report No. LBL-12219 (unpublished).
 - [24] H. Daniel and G. W. Eakins, Phys. Rev. **117**, 1565 (1960).
 - [25] B. N. Subba Rao, Nuovo Cimento **20**, 178 (1961).
 - [26] Z. W. Grabowski, R. S. Raghavan, and R. M. Steffen, Phys. Rev. **139**, B24 (1965).
 - [27] K. S. R. Sastry, R. J. Ouellette, Y. Sharma, and R. Strange, Phys. Lett. **26B**, 207 (1968).